ACS APPLIED BIO MATERIALS

www.acsabm.org Article

Quantifying Bound Proteins on Pegylated Gold Nanoparticles Using Infrared Spectroscopy

Paul R. Handali and Lauren J. Webb*

Cite This: https://doi.org/10.1021/acsabm.4c00012 Read Online

ACCESS | Metrics & More | Article Recommendations | Supporting Information

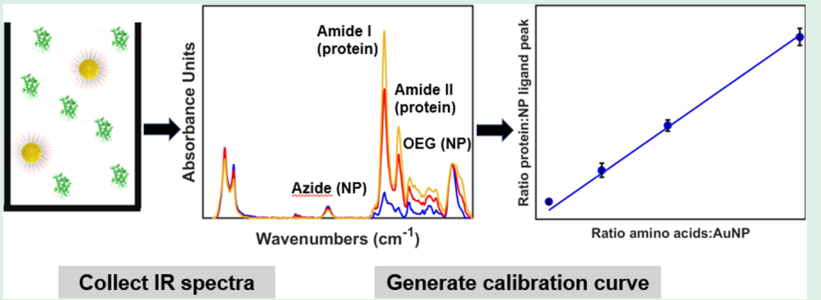

ABSTRACT: Protein−nanoparticle (NP) complexes are nanomaterials that have numerous potential uses ranging from biosensing to biomedical applications such as drug delivery and nanomedicine. Despite their extensive use quantifying the number of bound proteins per NP remains a challenging characterization step that is crucial for further developments of the conjugate, particularly for metal NPs that often interfere with standard protein quantification techniques. In this work, we present a method for quantifying the number of proteins bound to pegylated thiol-capped gold nanoparticles (AuNPs) using an infrared (IR) spectrometer, a readily available instrument. This method takes advantage of the strong IR bands present in proteins and the capping ligands to quantify protein−NP ratios and circumvents the need to degrade the NPs prior to analysis. We show that this method is generalizable where calibration curves made using inexpensive and commercially available proteins such as bovine serum albumin (BSA) can be used to quantify protein−NP ratios for proteins of different sizes and structures.

KEYWORDS: *protein quantification, infrared spectroscopy, nanoparticle functionalization, bioconjugation, protein−nanoparticle characterization*

INTRODUCTION

Nanoparticles (NPs) have been shown to be effective scaffolds on which stable and active proteins and enzymes can be immobilized.[1−6] Characterization of proteins grafted onto NPs is crucial to the development of these protein-based nanomaterials. Some common and important characterization parameters include activity, stability, and amount of bound protein.[7,8] Out of these important characteristics, the quantification of the amount of bound protein is one of the most important since it determines the efficiency of binding and the effects of binding on protein activity.[9−12] We recently surveyed the currently available methods to determine this quantity on NPs and the few available methods often require expertise and instrumentation that are not readily available.[9] Though measuring protein concentration in solution is straightforward and well established,[13] the presence of NPs makes this measurement significantly more challenging as NPs (particularly metal NPs) tend to interfere with the most common optical techniques used to determine protein concentration, UV−visible and fluorescence spectroscopies. NPs often absorb in the visible range of the electromagnetic spectrum (400−800 nm), thus interfering with common assays of protein concentration, structure, and function. Metal NPs are also strong quenchers of fluorescence, making one of the most ubiquitous assay measurement techniques unusable.[14,15] As a result, researchers have often resorted to etching away the NPs, thus leaving the proteins in the remnant solution to be measured.[16,17] However, this is not always possible if NPs are capped with densely packed ligands to help with solution stabilization and protect the NP structure from many etching agents.[18] Another approach has been to use amino acid analysis (AAA), a technique originally designed to determine amino acid composition of proteins that has more recently been applied to determine protein concentration with detection limits in the nM range.[10,19,20] This approach uses harsh conditions to both degrade the NP and hydrolyze the

Received: January 4, 2024
Revised: February 21, 2024
Accepted: February 26, 2024

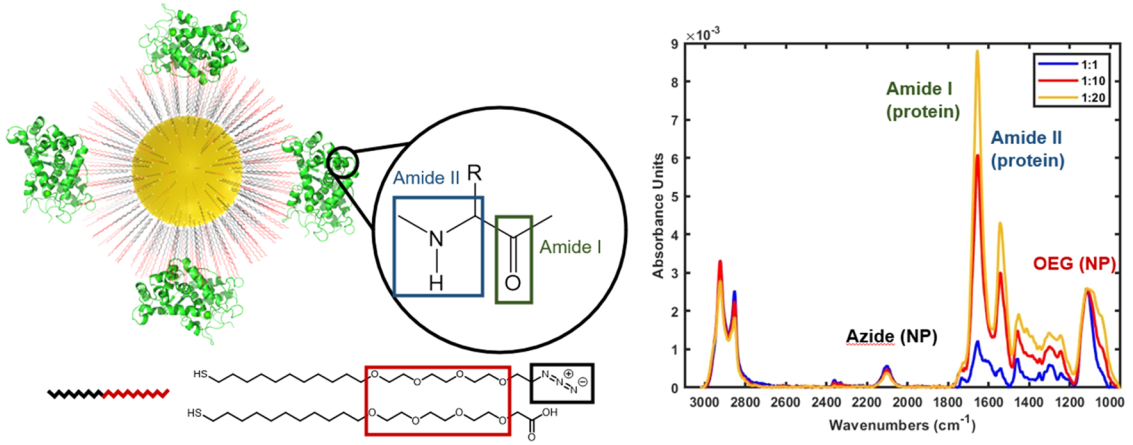

Figure 1. Scale model of HRP bound to AuNP ligands highlighting moieties of interest from the NP and the protein (left). Overlaid IR spectra of 1:1 (blue), 1:10 (red), and 1:20 (yellow) ratios of HRP/AuNP mixtures (right).

protein's peptide bonds, thus eliminating interference from NPs and allowing for derivatization and quantification of the amino acids in solution. However, higher concentrations of NPs have been shown to introduce background noise, and it is recommended that the protein of interest be used to make calibration curves, which is not ideal if the protein of interest is expensive or has limited availability. Because of these constraints, there are few techniques to quantify NP−protein interactions that are robust and reliable for a wide variety of systems of interest.

Infrared (IR) spectroscopy is a technique often used to characterize protein−NP materials.[5,21−23] For example, IR spectroscopy has been used to quantify ligands on NPs,[24−26] although it is often difficult to accommodate high limits of detection and variability in absolute absorbance between scans. However, including an internal standard in the measurement can significantly increase consistency, and using attenuated total internal reflection (ATR) IR to measure dry samples can increase the sensitivity. Proteins have strong and characteristic absorbance in the IR spectrum, particularly with the amide I and amide II bands at ∼1650 and ∼1540 cm^{-1} respectively.[27−29] Ligand-capped NPs also absorb in the IR. Pegylated thiols are commonly used capping ligands for NPs because they provide stability in aqueous solution, a key requirement for any NP material to be relevant to biological applications.[20,21,30−32] They have strong absorbance in the IR region, with the C−O band from the oligoethylene glycol (OEG) moieties absorbing at ∼1100 cm^{-1}. There are also commercially available variants of these pegylated thiols that facilitate the addition of other functional groups to less cluttered regions of the spectrum. One example is azide-terminated thiols, often used for binding NPs to proteins through click chemistry.[20,33−35] Azide moieties absorb at ∼2100 cm^{-1} which is usually an empty region in a protein IR spectrum, thus making it relatively free from interference. Indeed, there is also precedent in using the difference in the azide peak height before and after functionalization to determine the yield of bioconjugation.[20] These OEG and azide peaks are proportional to NP concentration, and ratios of these peaks to the protein amide peaks should be indicative of the ratio of proteins to NPs. Finding such a convenient and noninterfering molecular absorption allows for quantification of bound proteins per NP using IR spectroscopy without the need for digestion of the NPs, but rather using them as an inherent internal standard to calibrate the measurement (Figure 1). If performed in solution, this method could also allow for the nondestructive analysis of rare samples before other experiments are conducted.

In this work, we demonstrate a method using IR spectroscopy to quantify bound proteins on pegylated thiol-capped gold nanoparticles (AuNPs) in a nondestructive way. We chose AuNPs because they are the most widely used NPs due to their stability and variety of potential applications.[36−39] The azide and OEG IR bands of the AuNP capping ligands were used as internal standard references, and the ratio of the protein amide I and amide II bands to the NP-ligand bands was correlated to the ratio of protein to AuNP. We show that this method is generalizable, where a cheap and commercially available protein can be used to make a reliable calibration curve usable for any protein−AuNP complex. We performed AAA to compare and calibrate our results with a well-established analytical method. Finally, we report an application of this technique in which we covalently bound proteins to AuNPs and determined the number of bound enzymes per AuNP.

MATERIALS AND METHODS

H_2SO_4, NaOH, NaCl, Na_2HPO4, 2-(*N*-morpholino) ethanesulfonic acid (MES), 4-(2-hydroxyethyl)-1-piperazineethanesulfonic acid (HEPES), ethanol, and toluene were purchased from Fisher Scientific. 1-Ethyl-3-(3′-dimethyaminopropyl) carbodiimide HCl (EDC), sulfo-*N*-hydroxysuccinimide (sulfo-NHS), 4-(dimethylamino) pyridine (DMAP), tetraocetylammonium bromide (TOAB), picrylsulfonic acid, $HAuCl_4$, $NaBH_4$, horseradish peroxidase (HRP), bovine serum albumin (BSA), cytochrome C (Cyt C), and Amicon Ultra 0.5 mL, 30 and 100 kDa molecular weight cutoff filters were purchased from Millipore Sigma. SH-C_{11}−OEG_3-COOH was purchased from Biochempeg and SH-C_{11}−OEG_4-N_3 was purchased from Prochimia Surfaces.

Synthesis of AuNP−Protein Conjugates. AuNPs with SH-C11-$(OEG)_4$-X (X = N_3, COOH) ligands (hereafter called "AuNP-N_3/COOH") were synthesized using a previously published procedure.[5,21] Briefly, an aqueous solution of $HAuCl_4$ (0.142 M, 1 mL) was added to a solution of TOAB (0.030 M, 10 mL) and stirred for 30 min until the solution turned dark brown. An aqueous solution of $NaBH_4$ (1.5 M, 1 mL) was quickly added and left to stir overnight, turning dark purple minutes after the addition of $NaBH_4$. The solution was then transferred to a separatory funnel and washed 3× with 0.1 M H_2SO_4, 0.1 M NaOH, and deionized water, and the aqueous layer was discarded. An aqueous solution of DMAP (0.1 M,

https://doi.org/10.1021/acsabm.4c00012
ACS Appl. Bio Mater. XXXX, XXX, XXX−XXX

10 mL) was added to the separatory funnel and mixed vigorously for 5 min, until the AuNPs transferred to the aqueous phase. The aqueous layer was collected and stored in the dark for further use.

Solutions of SH-C_{11}-$(OEG)_3$-COOH (10 mM, 525 μL) and SH-C_{11}-$(OEG)_4$-N_3 (10 mM, 175 μL) in EtOH were mixed and added to solutions of DMAP-capped AuNPs (2.5 mL, 1.15 μM) and left overnight to form AuNP-N_3/COOH. These AuNP-N_3/COOH were then spun 8× at 14,000 g for 10 min using 30 kDaA Amicon MWCO filters to remove free thiols. The AuNP-N_3/COOH were reconstituted in 3 mL of pH 5 MES and stored in the dark until further use. Transmission electron microscopy (TEM, JEOL 2010 F) was used to measure the size distribution of the AuNPs (n = 100).

To bind Cyt C and BSA to AuNP-N_3/COOH, EDC/NHS cross-linking chemistry was used to bind free lysines to the COOH ligands on the AuNPs. To a solution of AuNP-N_3/COOH (125 μL, 1.15 μM) in pH 5 MES was added 47.9 mg of EDC (0.25 mmol) and 108 mg of sulfo-NHS (0.5 mmol) and shaken at 1000 rpm for 15 min. The AuNP-N_3/COOH was then spun three times at 14,000 g in 100 kDa MWCO filters for 5 min to remove excess reagents. The activated AuNP-N_3/COOH were then added to 200 μL of 14.4 μM BSA and Cyt C in 10 mM pH 8 HEPES and left to shake overnight at 1000 rpm. The AuNP−protein conjugates were then spun 10 times at 14,000 g and 4 °C for 3 min with 100 kDa MWCO filters to remove unbound protein. The samples were then buffer-switched to HPW using 100 kDa MWCO filters and then analyzed by ATR-IR spectroscopy.

Infrared Spectroscopy. Concentrations of AuNP-N_3/COOH and protein solutions were determined using UV−vis (Agilent) spectroscopy measuring absorbance at 506 nm (ε = 8.6 × 10^6 M^{-1} cm^{-1} for AuNPs)[40] and 280 nm, respectively. Solutions of 0.5 μM AuNP-N_3/COOH in HPW were mixed with solutions of HRP, BSA, and Cyt C in varying protein/AuNP ratios. The mixtures were then drop-cast onto the Ge ATR crystal (Harrick), and scans were taken once the sample was dry using a Vertex 70 IR Spectrometer (Bruker). A total of 1000 scans were taken per sample at 4 cm^{-1} resolution. The spectra were blank-subtracted with a spectrum of a clean crystal and normalized by the C−O stretching band at 1120 cm^{-1} using the instrument's OPUS software (Bruker). Each measurement was performed in triplicate.

Amino Acid Analysis. Solutions of varying concentrations of HRP, BSA, and Cyt C were used to make three separate calibration curves for each protein. To each of these solutions was added 100 μL of 6 M HCl, which were then placed in a heating block at 110 °C and left for 24 h in closed PCR tubes. The lids were then opened, and the water was evaporated, after which the residue was reconstituted in 100 μL of pH 8.5 sodium bicarbonate buffer. The solutions were transferred to a clear flat-bottom 96-well plate, and 50 μL of 0.01% TNBS was added to each well. The well was incubated at 37 °C for 2 h, after which 50 μL of 10% SDS solution was added. Absorbance at 420 nm was then measured on a Synergy H4 plate reader (BioTek), with each assay performed in triplicate.

Statistical Analysis for Regression Line Comparison. Comparison between two linear slopes was performed using a procedure outlined by Andrade et al.[41] Slopes of two lines were compared using a Student's t-test where n = 4 with $2n - 2$ degrees of freedom. For two lines with equations $y_1 = m_1x_1$ and $y_2 = m_2x_2$, the parameter t was calculated using eq 1

$$t = \frac{m_1 - m_2}{\sqrt{s^2\left(\frac{1}{\delta x_1(n-1)} + \frac{1}{\delta x_2(n-1)}\right)}} \quad (1)$$

where δx_1 and δx_2 represent the standard deviation in x for each line, respectively, and s^2 is the common residual variance between the two regressions. s^2 is given by eq 2

$$s^2 = \frac{n - 1({s_1}^2 + {s_2}^2)}{2n - 2} \quad (2)$$

where s_1 and s_2 represent the standard error for the y estimate for each line, respectively. For this report, two slopes were considered statistically significant when $t > 3.71$ ($p < 0.01$).

RESULTS AND DISCUSSION

HRP, BSA, and Cyt C were chosen for this study because they are commonly used proteins as model protein systems, are useful for various applications, and are commercially available.[42,43] They are also of varying sizes (44, 66, and 14 kDa respectively), thus allowing us to test the generalizability of this method. The capping ligand SH-C_{11}-$(OEG)_3$-COOH for the AuNPs was selected because pegylated thiols provide stability for AuNPs in aqueous solution while also containing a carboxyl tail, which is often used to bind enzymes to NPs. The characteristic C−O peak at 1120 cm^{-1} from the OEG group was used as a reference peak in the IR spectrum to determine the ratio of the enzyme to AuNPs. The azide variant was selected to provide a reference peak in the IR spectrum generally free of potential peak interference that would correlate to the amount of AuNPs (Figure 1). The AuNPs used in this study were determined to have Au core sizes of 4.8 ± 1.1 nm using TEM though this method can be applied to NPs of different core sizes. We will discuss the potential applications and limitations of this technique in detail in a later section.

To construct calibration curves, we made solutions of AuNP-N_3/COOH and each protein, where the AuNP-N_3/COOH concentration was held constant and the protein concentration was varied. The ratio of protein to AuNP-N_3/COOH in each calibration standard was known from the measurement of the concentrations of each protein measured separately by using UV−visible spectroscopy. The standards were then analyzed using IR spectroscopy. The characteristic amide I and amide II bands at 1656 and 1540 cm^{-1}, respectively, were used to quantify the amount of protein, while the C−O and azide bands at 1120 and 2103 cm^{-1}, respectively, were used to quantify the amount of AuNP.[20,29] We then plotted the ratios of these peaks against the known values in the calibration standards to generate a calibration curve. To determine the generalizability of this method, we plotted these peak ratios as a function of the ratio of the total number of amino acids to AuNP-N_3/COOH (Figure 1). The peptide bonds in the amino acids are the main contributors to the amide peak heights, and so the ratio of the amide peak heights to the NP peak heights should correlate linearly with respect to the ratio of amino acids to AuNP-N_3/COOH.[27−29] We hypothesized that using this ratio would result in similar if not identical calibration curves for the different proteins, thus potentially allowing us to use a calibration curve generated using one protein to determine the protein/AuNP ratio of any protein−AuNP complex. We arbitrarily chose amino acid/AuNP ratios that corresponded to the following ratios of HRP/AuNP: 1:1, 5:1, 10:1, and 20:1, resulting in amino acid/AuNP ratios of 308:1, 1540:1, 3080:1, and 6160:1, respectively. We chose the following peak ratios to analyze: amide I/OEG, amide I/azide, and amide II/azide since these are the most prominent and distinguishable peaks in the IR spectrum that are indicative of the protein/AuNP ratio.

OEG as Reference Peak. We chose azide-terminated pegylated thiols for the AuNP capping ligand because they are frequently used for binding NPs to proteins and small molecules through azide−alkyne click chemistry, are well characterized, and are readily available for this purpose.

https://doi.org/10.1021/acsabm.4c00012
ACS Appl. Bio Mater. XXXX, XXX, XXX−XXX

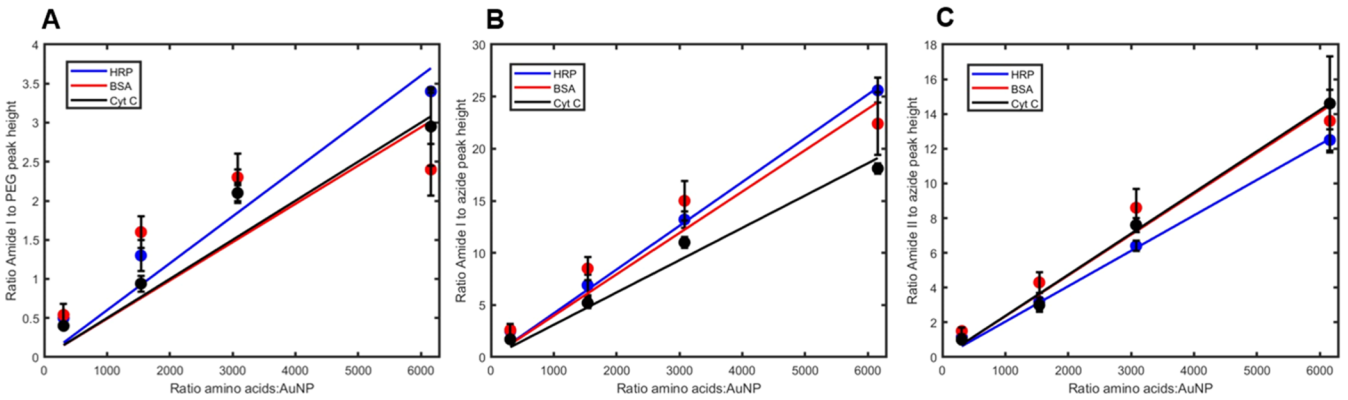

Figure 2. Calibration curves of ratios of IR HRP (blue), BSA (red), and Cyt C (black) peaks to AuNP peaks. (A) Ratio of amide I to PEG peak height, (B) ratio of amide I to azide peak height, and (C) ratio of amide II to azide peak height, all as a function of ratio of amino acids per NP. Error bars indicate standard deviation where $n = 3$.

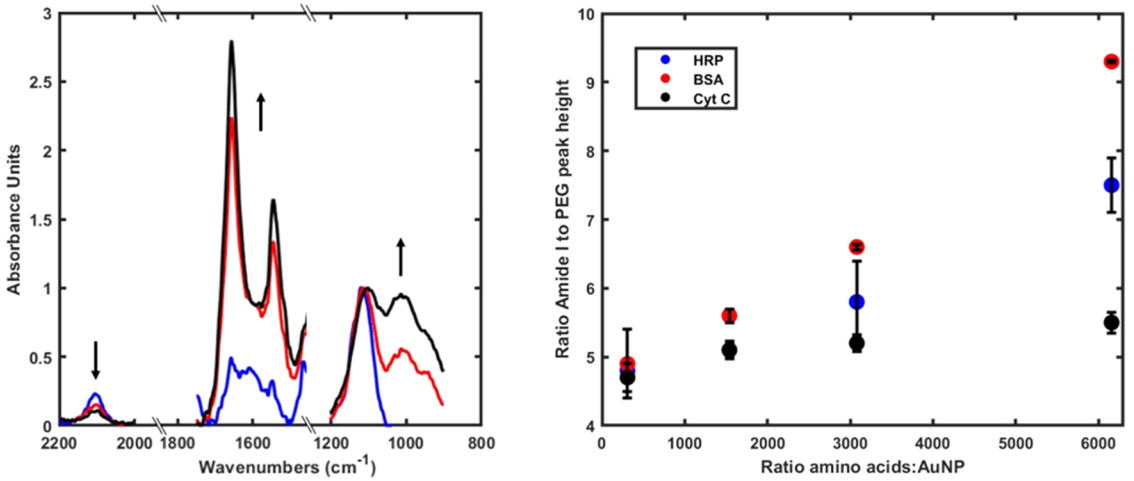

Figure 3. (Left) representative overlaid IR spectra for mixtures of increasing ratios of BSA to AuNP (1:1 (blue), 10:1 (red), and 20:1 (black)). Arrows highlight increases in PEG and amide peaks and decreases in azide peaks. (Right) Ratio of the PEG/azide peaks plotted as a function of the ratio of amino acids to AuNP for HRP (blue), BSA (red), and Cyt C (black). Error bars indicate standard deviation where $n = 3$.

Plotting the ratios of the amide I/OEG peaks as a function of amino acid/AuNP ratios for HRP, BSA, and Cyt C resulted in linear calibration curves (Figure 2A), demonstrating that pegylated ligands can be used to determine protein/AuNP ratios. One exception is the final data point in the BSA curve. This is due to a peak at ~1000 cm^{-1} that increases with an increased amount of added BSA and that interferes with the C−O band at 1120 cm^{-1} (Figure 3). Similar but significantly smaller interference was observed with HRP, likely from sugars bound to HRP due to glycosylation,[44] but these had a minimal effect on the linearity of the calibration curve. This trend was observed by plotting the ratio of the OEG/azide peaks as a function of the AA/AuNP ratio, where for BSA and HRP, the OEG peak increased with protein concentration while it remained constant for Cyt C with no observed interference (Figure 3). These interferences, however, were absent in the spectra of BSA covalently bound to AuNP-N_3/COOH (Figure S1). These AuNP-BSA complexes were buffer-exchanged into HPW prior to IR analysis. The calibration standards were made by dissolving lyophilized BSA powder (which includes buffer salts) into HPW and directly mixing it with AuNP-N_3/COOH in HPW without further sample prep. It is therefore likely that the interference in the IR spectra of the calibration standards is a result of these buffer salts, most likely phosphate salts. In contrast, lyophilized HRP and Cyt C powders were salt-free and thus did not present significant interference. We attempted to move BSA into HPW with Amicon MWCO filters for more representative calibration standards, but this resulted in BSA and AuNP-N_3/COOH precipitating from the solution. It is important to note that this did not occur when buffer-exchanging AuNP-bound BSA, indicating that covalent binding to the AuNP-N_3/COOH imparted further stability to the BSA.[5,45] BSA is a representative case, as precipitation in the absence of buffer salts is a likely occurrence for many proteins of interest. This issue of buffer salts interfering with measurements can be circumvented by using different peaks in the IR spectrum (as will be discussed later), and thus, the instability of a protein in HPW does not affect generalizability of this method. While the C−O band is useful and capable of performing this analysis, it absorbs in a cluttered region in the IR spectrum and can be prone to interference. Therefore, in circumstances where there is significant interference, an additional moiety can be added that absorbs in a clean part of the IR spectrum.

Azide as Reference Peak. Using the azide peak as the reference AuNP-N_3/COOH peak eliminates the deviation observed using the C−O stretching band, resulting in three linear calibration curves in which HRP and BSA had nearly

https://doi.org/10.1021/acsabm.4c00012
ACS Appl. Bio Mater. XXXX, XXX, XXX−XXX

identical results. Cyt C however had a shallower slope. Although the differences between the slopes of the three curves were calculated to be statistically insignificant (Table S1), this observation highlights one issue with using amide I as the reference protein peak (Figure 2B). The peak height and shape of the amide I band in proteins is heavily influenced by secondary structure, and as a result simply using peak height would not be generalizable across different proteins.[27−29] It should be noted that amide I is indeed frequently used to measure changes in the secondary structure of proteins.[45] The peak used for this analysis was at 1656 cm^{-1}, which is representative of an α-helical secondary structure. HRP, BSA, and Cyt C all have primarily α-helical secondary structure as can be seen from their crystal structures, yet Cyt C has a lower peak height at 1656 cm^{-1} and thus has a shallower slope.[46−48] One possible explanation for this is that Cyt C undergoes more unfolding than HRP and BSA when drop-cast and dried on the ATR crystal, thus lowering the peak height to 1656 cm^{-1}. Fitting and plotting areas under the curve could potentially align the slopes of each curve, but this is convoluted by overlapping peaks such as the carbonyl stretch from the AuNP-N_3/COOH carboxyl group as well as with amide II. To compensate for the effects of secondary structure on amide I, we then used the ratio of amide II to azide (Figure 2C). Amide II is a band that is not influenced by secondary structure and is consistent among different proteins.[28,29] Plotting this ratio against known AA/AuNP ratios for HRP, BSA, and Cyt C resulted in three nearly identical curves with statistically insignificant differences (Table S1). This shows that the amide II and azide peaks are the most generalizable across different proteins and thus can potentially be used to determine the protein/AuNP ratio for any protein−AuNP complex. However, amide II bands are not as intense as amide I bands and, because of this lower sensitivity, are not recommended for quantifying the amount of protein for complexes with low protein−AuNP ratios.

Determining the Number of Bound Proteins to AuNP-N_3/COOH. To see if this analytical procedure can be used on actual protein−NP complexes, we used EDC/NHS cross-linking chemistry, a commonly used bioconjugation reaction,[5,49−51] to bind BSA and Cyt C to AuNP-N_3/COOH (making AuNP-BSA and AuNP-Cyt C), and analyzed the samples using IR. To validate our results, we also performed amino acid analysis (AAA) on these bioconjugated constructs. AAA is a well-established and reliable method that has been used to quantify the number of proteins bound per AuNP-N_3/COOH.[10,19,20] Briefly, samples are boiled in 6 M HCl to hydrolyze the peptide bonds, resulting in free amino acids in solution. This process also dissolves the NPs and eliminates potential interference in subsequent spectroscopic measurement. The amino acids are then labeled with the chromophore TNBS and absorbance at 420 nm is measured. Calibration curves were made for HRP, BSA, and Cyt C, where absorbance at 420 nm was plotted as a function of the number of amino acids in nmol (Figure 4). Like the results from IR spectroscopy discussed above, using equivalent nanomoles of amino acids between the three proteins yielded calibration curves of similar slopes. However, there is more variance in the y-intercepts of the fits, which suggests that different proteins have varying levels of background absorbance not accounted for by background subtraction.

To quantify bound protein per AuNP-N_3/COOH using IR, we buffer-exchanged AuNP-BSA and AuNP-Cyt C into HPW and drop-cast the solutions onto a Ge ATR crystal. Once dry, we collected spectra and used the ratio of the amide II and azide peak intensities since, as discussed previously, those were the two most consistent peaks among the proteins we investigated. Taking the ratio of the amide II peak height to the azide peak height, we used linear regression to then calculate the number of amino acids per AuNP-N_3/COOH using the calibration curves shown in Figure 2C. This value was then divided by the number of amino acids in the respective protein (104 for Cyt C, 583 for BSA)[47,48] to determine the number of Cyt C and BSA per AuNP-N_3/COOH. We compared the protein−AuNP ratios determined using all three calibration curves for each AuNP−protein complex to determine the generalizability of this method (Table 1). Using the calibration curves generated using HRP, BSA, and Cyt C respectively, we determined nearly identical protein−AuNP ratios for AuNP-bound BSA (6.3 ± 0.8, 5.4 ± 0.7, and 5.4 ± 0.7 BSA/AuNP) and AuNP-bound Cyt C (10.4 ± 0.9, 9.0 ± 0.8, and 8.9 ± 0.8 Cyt C/AuNP), demonstrating consistency in the results across the three proteins. Most notably, protein quantities obtained from the BSA and Cyt C calibration curves were identical. Since BSA and Cyt C have different sizes (66 and 14 kDa respectively) and secondary structures, this shows that a commonly available protein like BSA or HRP can be used to measure the protein/AuNP ratio of a variety of structurally different proteins bound to AuNPs. To validate these results, we compared them to those determined from AAA. We used the calibration curve of the respective protein (i.e., the Cyt C calibration curve for Cyt C

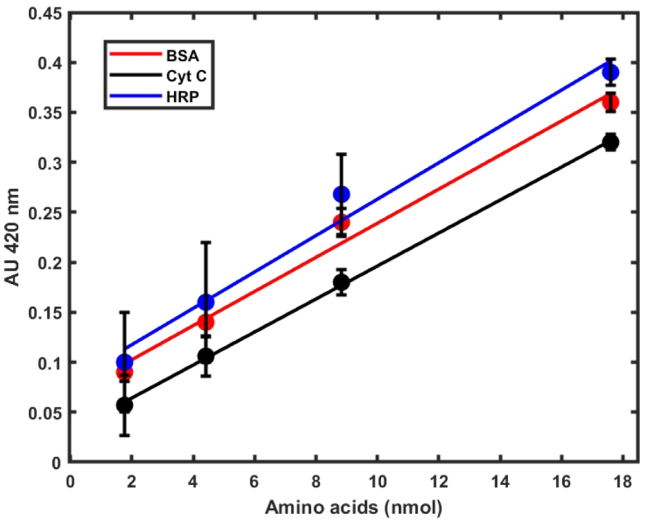

Figure 4. Overlaid calibration curves generated using amino acid analysis on HRP (blue), BSA (red), and Cyt C (black) with absorbance at 420 nm plotted as a function of number of amino acids (nmol). Error bars indicate standard deviation where n = 3.

Table 1. Quantity of Protein Bound Per AuNP Determined Using IR and AAA

	IR (amide II/azide ratio curves)			amino acid analysis
	HRP curve	BSA curve	Cyt C curve	
BSA/AuNP	6.3 ± 0.8	5.4 ± 0.7	5.4 ± 0.7	4.6 ± 0.2
Cyt C/AuNP	10.4 ± 0.9	9.0 ± 0.8	8.9 ± 0.8	6.6 ± 0.14

https://doi.org/10.1021/acsabm.4c00012
ACS Appl. Bio Mater. XXXX, XXX, XXX−XXX

and the BSA calibration curve for BSA), yielding protein quantities of 6.6 ± 0.14 Cyt C/AuNP and 4.6 ± 0.2 BSA/AuNP. These values are slightly lower than those determined by IR. One hypothesis for why AAA results in lower quantified protein is that the presence of the AuNP could reduce the efficiency of the sample hydrolysis, thus resulting in fewer amino acids in solution and slightly underestimating the number of bound proteins. However, the differences between the results from the two methods are still marginal, with spectroscopic analysis having the significant advantage of being nondestructive.

Practical Guidelines. In this section, we offer guidelines for both sample handling and for analysis. For the AuNPs used in this work, we drop-cast 10 μL of 0.5 μM AuNP onto the ATR crystal and allow it to dry before running the scan. This is equivalent to ~0.2 μg of protein assuming a 1:1 ratio of AuNP to protein. We would not recommend using concentrations lower than this, as spectra of AuNPs and proteins at concentrations lower than this have considerably higher noise levels and could result in higher error. However, it is possible to see all of the NP peaks for a sample of 10 μL of 0.1 μM AuNP drop-cast and dried on an ATR crystal so if necessary one can go as low as this (Figure S3). In terms of the lowest protein−AuNP ratios that can be detected, this is dependent on the size of the protein. We show a sample spectrum of a 1:1 mixture of AuNP-N_3/COOH and Cyt C to demonstrate this limit (Figure S4). Both amide peaks are distinct enough above the carbonyl peak from AuNP-N_3/COOH to be detectable, though barely so. Since Cyt C has 104 amino acids, this shows that for the AuNPs used in this work, it is not recommended to use this method to measure amino acid/AuNP ratios of less than 100:1. It must be noted that these guidelines are for the NPs in this work specifically and are not generalizable to all NPs of different size, shape, and material. As such, we recommend making calibration curves for each NP used. It must also be noted that specifically for functionalized NPs, the reliability of this method depends on consistency in the degree of functionalization. The absolute degree of functionalization will not affect the results as long as it is consistent between samples. In order to ensure this consistency, we strongly recommend that the NPs used to make the calibration curve experience the same synthesis and buffer conditions that the protein-bound NPs would experience. Different solvents have the potential to affect the ligand density on the NPs and thus introduce error into results.

We have determined that both the amide I and amide II bands can be used to generate calibration curves to determine protein/AuNP ratios when using OEG and azide peaks as references. C−O bands from the pegylated thiols can be used as a AuNP reference peak as pegylated thiols are commonly used to stabilize metal NPs in aqueous solution. However, these absorb in a noisy region of a typical IR spectrum and thus can be prone to interference from other vibrational modes. Thus, in cases where it is sufficiently difficult to isolate the C−O stretch, we recommend including another functional group, such as an azide, which absorbs in a less cluttered region of the IR spectrum. Furthermore, the decision to choose amide I or amide II bands for calibration depends on the circumstances of the particular protein being investigated. Amide I bands absorb more strongly than amide II bands and offer a higher sensitivity. In cases in which protein−AuNP ratios are low, amide I is recommended. However, amide I is susceptible to variation from differences in secondary structure that may convolute a simple ratio-based analysis, and thus one should consider using the protein of interest to make the calibration curve if possible. It must be noted that binding to an NP can also result in a change in the secondary structure of the protein and thus alter the amide I band. This change could potentially skew measurements made using amide I. We recommend using the amide II band in cases where the protein sample might be limited and there is a large enough protein/AuNP ratio because it is significantly less skewed by differences in protein secondary and tertiary structure and can be calibrated by readily available model proteins such as BSA or HRP to determine the protein/AuNP ratio.

Scope of Applicability and Potential Limitations. We present a method for quantifying bound proteins to ligand-capped AuNPs with three key advantages. First, sample prep is significantly simplified, as it does not require etching or removal of the NPs or degradation of the proteins. Second, it uses IR spectroscopy, which is a readily available technique with minimal expertise required. Third and most significantly, a cheap and commonly available protein such as BSA or HRP can be used to make a calibration curve that can quantify the protein−NP ratio for a rare protein−NP conjugate of interest, thus saving expensive and precious material. While we only performed this analysis using pegylated AuNPs, we hypothesize that this method would be broadly applicable to NPs of any type given that the concentration of the NP can be determined separately and the NP has identifiable bands in the IR spectrum.

There are specific limitations to this method, which we highlight here. This technique cannot be applied to protein−NP materials with multiple protein species, as differentiating between these species would be difficult using only IR spectroscopy. As such, this method's usage would be limited for measuring the number of bound proteins in a protein corona with a mixture of different proteins all bound to the NP, though if the proteins of interest are of similar size, an estimate could potentially be determined. This method was developed for protein−NP conjugates, where the protein sample is pure and the binding of the protein to the NP is controlled. For samples where hundreds of proteins are bound per NP, the signal of the protein will likely overwhelm the NP peaks and potentially limit the applicability of this method. This would depend on the degree of functionalization and the strength of the IR band for the NP. As mentioned earlier, this method requires the NP of interest to have identifiable IR bands that are not affected by the presence of a protein. In this work, we used PEG and azides as the reference peaks as they are commonly used ligands for NP functionalization, but the applicability of this strategy is not limited to these ligands.

SUMMARY AND CONCLUSIONS

In this work, we demonstrate a method to quantify the number of bound proteins on ligand-capped AuNPs using a straightforward application of IR spectroscopy. Using the peaks that correspond to proteins (amide I and amide II) and the AuNP ligands used here (C−O and azide), we demonstrate that the ratios between these peaks can be correlated to the ratio of proteins to AuNPs in solution, thus allowing one to quantify the number of bound proteins in a given protein−AuNP complex. Analyzing protein−AuNP mixtures using three different proteins, we made calibration curves correlating the protein−AuNP peak ratios to the ratio of amino acids to AuNPs. We used these calibration curves to

https://doi.org/10.1021/acsabm.4c00012
ACS Appl. Bio Mater. XXXX, XXX, XXX−XXX

quantify the number of bound proteins for two different protein−AuNP complexes and determined that using the peak ratio of amide II to azide is the most consistent and reliable. We validated these results by comparing them to amino acid analysis, a well-established but destructive quantification method, and showed that both techniques produce comparable measurements of the number of proteins per NP. While this work was limited to ligand-capped AuNPs, the principle should still be applicable to NPs of different compositions provided the concentration of the NPs in solution can be determined separately. This method can be used broadly, requires no special instrumentation or expertise in IR spectroscopy, and is widely applicable to any NP-ligand construct that has identifiable bands in the IR spectrum. Most importantly, we showed that commonly available proteins like BSA and HRP can be used to accurately quantify the protein−AuNP ratio for a different protein−AuNP complex, making this a generalizable method and is particularly useful when the protein of interest is difficult to obtain.

■ ASSOCIATED CONTENT

Supporting Information

The Supporting Information is available free of charge at https://pubs.acs.org/doi/10.1021/acsabm.4c00012.

IR spectrum of AuNP-bound BSA; statistical values for curve comparison; TEM image of AuNP-N_3/COOH; IR spectrum of 0.1 μM AuNP-N_3/COOH; and IR spectrum of solution with 1:1 ratio of Cyt C and AuNP-N_3/COOH (PDF)

■ AUTHOR INFORMATION

Corresponding Author

Lauren J. Webb − *Department of Chemistry, Texas Materials Institute, and Interdisciplinary Life Sciences Program, The University of Texas at Austin, Austin, Texas 78712-1224, United States;* orcid.org/0000-0001-9999-5500; Email: lwebb@cm.utexas.edu

Author

Paul R. Handali − *Department of Chemistry, The University of Texas at Austin, Austin, Texas 78712-1224, United States*

Complete contact information is available at: https://pubs.acs.org/10.1021/acsabm.4c00012

Notes

The authors declare no competing financial interest.

■ ACKNOWLEDGMENTS

This work was supported by NSF (CHE-2203414). The authors gratefully acknowledge the UT-Austin Texas Materials Institute for the use of their facilities.

■ REFERENCES

(1) Sharma, S.; Gupta, S.; Princy; Arya, S. K.; Kaur, A. Enzyme Immobilization: Implementation of Nanoparticles and an Insight into Polystyrene as the Contemporary Immobilization Matrix. *Process Biochem.* **2022**, *120*, 22−34.

(2) Mitchell, M. J.; Billingsley, M. M.; Haley, R. M.; Wechsler, M. E.; Peppas, N. A.; Langer, R. Engineering Precision Nanoparticles for Drug Delivery. *Nat. Rev. Drug Discovery* **2021**, *20*, 101−124.

(3) Spicer, C. D.; Jumeaux, C.; Gupta, B.; Stevens, M. M. Peptide and Protein Nanoparticle Conjugates: Versatile Platforms for Biomedical Applications. *Chem. Soc. Rev.* **2018**, *47*, 3574−3620.

(4) Pollok, N. E.; Rabin, C.; Smith, L.; Crooks, R. M. Orientation-Controlled Bioconjugation of Antibodies to Silver Nanoparticles. *Bioconjugate Chem.* **2019**, *30*, 3078−3086.

(5) Handali, P. R.; Webb, L. J. Gold Nanoparticles Are an Immobilization Platform for Active and Stable Acetylcholinesterase: Demonstration of a General Surface Protein Functionalization Strategy. *ACS Appl. Bio Mater.* **2023**, *6* (1), 209−217.

(6) Xu, W.; He, W.; Du, Z.; Zhu, L.; Huang, K.; Lu, Y.; Luo, Y. Functional Nucleic Acid Nanomaterials: Development, Properties, and Applications. *Angew. Chem., Int. Ed.* **2021**, *60* (13), 6890−6918.

(7) Sapsford, K. E.; Tyner, K. M.; Dair, B. J.; Deschamps, J. R.; Medintz, I. L. Analyzing Nanomaterial Bioconjugates: A Review of Current and Emerging Purification and Characterization Techniques. *Anal. Chem.* **2011**, *83*, 4453−4488.

(8) Moreira-Alvarez, B.; Cid-Barrio, L.; Ferreira, H. S.; Costa-Fernández, J. M.; Encinar, J. R. Integrated Analytical Platforms for the Comprehensive Characterization of Bioconjugated Inorganic Nanomaterials Aiming at Biological Applications. *J. Anal. At. Spectrom.* **2020**, *35*, 1518−1529.

(9) Correira, J. M.; Handali, P. R.; Webb, L. J. Characterizing Protein−Surface and Protein−Nanoparticle: Activity, Binding, and Structure. *J. Chem. Phys.* **2022**, *157*, No. 090902.

(10) Oliverio, R.; Liberelle, B.; Murschel, F.; Garcia-Ac, A.; Banquy, X.; De Crescenzo, G. Versatile and High-Throughput Strategy for the Quantification of Proteins Bound to Nanoparticles. *ACS Appl. Nano Mater.* **2020**, *3* (10), 10497−10507.

(11) Schneck, N. A.; Phinney, K. W.; Lee, S. B.; Lowenthal, M. S. Quantification of Antibody Coupled to Magnetic Particles by Targeted Mass Spectrometry. *Anal. Bioanal. Chem.* **2016**, *408*, 8325−8332.

(12) Fernández-Iglesias, N.; Bettmer, J. Complementary Mass Spectrometric Techniques for the Quantification of the Protein Corona: A Case Study on Gold Nanoparticles and Human Serum. *Nanoscale* **2015**, *7*, 14324−14331.

(13) Sapan, C. V.; Lundblad, R. L. Review of Methods for Determination of Total Protein and Peptide Concentration in Biological Samples. *Proteomics: Clin. Appl.* **2015**, *9* (3−4), 268−276.

(14) Pustovit, V. N.; Shahbazyan, T. V. Fluorescence Quenching near Small Metal Nanoparticles. *J. Chem. Phys.* **2012**, *136*, No. 204701.

(15) Dulkeith, E.; Morteani, A. C.; Niedereichholz, T.; Klar, T. A.; Feldmann, J.; Levi, S. A.; Van Veggel, F. C. J. M.; Reinhoudt, D. N.; Möller, M.; Gittins, D. I. Fluorescence Quenching of Dye Molecules near Gold Nanoparticles: Radiative and Nonradiative Effects. *Phys. Rev. Lett.* **2002**, *89*, No. 203002.

(16) Zhang, L.; Hu, D.; Salmain, M.; Liedberg, B.; Boujday, S. Direct Quantification of Surface Coverage of Antibody in IgG-Gold Nanoparticles Conjugates. *Talanta* **2019**, *204*, 875−881.

(17) Filbrun, S. L.; Driskell, J. D. A Fluoresence-Based Method to Directly Quantify Antibodies Immobilized on Gold Nanoparticles. *Analyst* **2016**, *141*, 3851−3857.

(18) Mei, B. C.; Oh, E.; Susumu, K.; Farrell, D.; Mountziaris, T. J.; Mattoussi, H. Effects of Ligand Coordination Number and Surface Curvature on the Stability of Gold Nanoparticles in Aqueous Solutions. *Langmuir* **2009**, *25* (18), 10604−10611.

(19) Liu, S.; Horak, J.; Höldrich, M.; Lämmerhofer, M. Accurate and Reliable Quantification of the Protein Surface Coverage on Protein-Functionalized Nanoparticles. *Anal. Chim. Acta* **2017**, *989*, 29−37.

(20) Wilder, L. M.; Handali, P. R.; Webb, L. J.; Crooks, R. M. Interactions between Oligoethylene Glycol-Capped AuNPs and Attached Peptides Control Peptide Structure. *Bioconjugate Chem.* **2020**, *31*, 2383−2391.

(21) Wilder, L. M.; Fies, W. A.; Rabin, C.; Webb, L. J.; Crooks, R. M. Conjugation of an α-Helical Peptide to the Surface of Gold Nanoparticles. *Langmuir* **2019**, *35* (9), 3363−3371.

(22) López-Lorente, Á. I.; Mizaikoff, B. Recent Advances on the Characterization of Nanoparticles Using Infrared Spectroscopy. *TrAC, Trends Anal. Chem.* **2016**, *84*, 97−106.

(23) Tsai, D.-H.; Davila-Morris, M.; Delrio, F. W.; Guha, S.; Zachariah, M. R.; Hackley, V. A. Quantitative Determination of Competitive Molecular Adsorption on Gold Nanoparticles Using Attenuated Total ReflectanceÀFourier Transform Infrared Spectroscopy. *Langmuir* **2011**, *27*, 9302−9313.
(24) Xu, H.; Yan, F.; Monson, E. E.; Kopelman, R. Room-Temperature Preparation and Characterization of Poly (Ethylene Glycol)-Coated Silica Nanoparticles for Biomedical Applications. *J. Biomed. Mater. Res., Part A* **2003**, *66A* (4), 870−879.
(25) Zhou, H.; Li, X.; Lemoff, A.; Zhang, B.; Yan, B. Structural Confirmation and Quantification of Individual Ligands from the Surface of Multi-Functionalized Gold Nanoparticles. *Analyst* **2010**, *135*, 1210−1213.
(26) Davis, K.; Cole, B.; Ghelardini, M.; Powell, B. A.; Mefford, O. T. Quantitative Measurement of Ligand Exchange with Small-Molecule Ligands on Iron Oxide Nanoparticles via Radioanalytical Techniques. *Langmuir* **2016**, *32* (51), 13716−13727.
(27) López-Lorente, Á. I.; Mizaikoff, B. Mid-Infrared Spectroscopy for Protein Analysis: Potential and Challenges. *Anal. Bioanal. Chem.* **2016**, *408*, 2875−2889.
(28) Barth, A. Infrared Spectroscopy of Proteins. *Biochim. Biophys. Acta, Bioenerg.* **2007**, *1767*, 1073−1101.
(29) Yang, H.; Yang, S.; Kong, J.; Dong, A.; Yu, S. Obtaining Information about Protein Secondary Structure in Aqueous Solution Using Fourier Transfor IR Spectroscopy. *Nat. Protoc.* **2015**, *10* (3), 382−396.
(30) Shi, L.; Zhang, J.; Zhao, M.; Tang, S.; Cheng, X.; Zhang, W.; Li, W.; Liu, X.; Peng, H.; Wang, Q. Effects of Polyethylene Glycol on the Surface of Nanoparticles for Targeted Drug Delivery. *Nanoscale* **2021**, *13*, 10748−10764.
(31) Yadav, D.; Dewangan, H. K. PEGYLATION: An Important Approach for Novel Drug Delivery System. *J. Biomater. Sci., Polym. Ed* **2021**, *32* (2), 266−280.
(32) Sur, S.; Rathore, A.; Dave, V.; Reddy, K. R.; Chouhan, R. S.; Sadhu, V. Recent Developments in Functionalized Polymer Nanoparticles for Efficient Drug Delivery System. *Nano-Struct. Nano-Objects* **2019**, *20*, No. 100397.
(33) Sapsford, K. E.; Algar, W. R.; Berti, L.; Gemmill, K. B.; Casey, B. J.; Oh, E.; Stewart, M. H.; Medintz, I. L. Functionalizing Nanoparticles with Biological Molecules: Developing Chemistries That Facilitate Nanotechnology. *Chem. Rev.* **2013**, *113* (3), 1904−2074.
(34) Scinto, S. L.; Bilodeau, D. A.; Hincapie, R.; Lee, W.; Nguyen, S. S.; Xu, M.; am ende, C. W.; Finn, M. G.; Lang, K.; Lin, Q.; Pezacki, J. P.; Prescher, J. A.; Robillard, M. S.; Fox, J. M. Bioorthogonal Chemistry. *Nat. Rev. Methods Primers* **2021**, *1*, No. 30.
(35) Furst, A. L.; Hill, M. G.; Barton, J. K. DNA-Modified Electrodes Fabricated Using Copper-Free Click Chemistry for Enhanced Protein Detection. *Langmuir* **2013**, *29* (52), 16141−16149.
(36) Malekzad, H.; Zangabad, P. S.; Mirshekari, H.; Karimi, M.; Hamblin, M. R. Noble Metal Nanoparticles in Biosensors: Recent Studies and Applications. *Nanotechnol. Rev.* **2017**, *6* (3), 301−329.
(37) Zhao, P.; Li, N.; Astruc, D. State of the Art in Gold Nanoparticle Synthesis. *Coord. Chem. Rev.* **2013**, *257*, 638−665.
(38) Nejati, K.; Dadashpour, M.; Gharibi, T.; Mellatyar, H.; Akbarzadeh, A. Biomedical Applications of Functionalized Gold Nanoparticles: A Review. *J. Cluster Sci.* **2022**, *33*, 1−16.
(39) Sani, A.; Cao, C.; Cui, D. Toxicity of Gold Nanoparticles (AuNPs): A Review. *Biochem. Biophys. Rep.* **2021**, *26*, No. 100991.
(40) Liu, X.; Atwater, M.; Wang, J.; Huo, Q. Extinction Coefficient of Gold Nanoparticles with Different Sizes and Different Capping Ligands. *Colloids Surf., B* **2007**, *58*, 3−7.
(41) Andrade, J. M.; Estévez-Pérez, M. G. Statistical Comparison of the Slopes of Two Regression Lines: A Tutorial. *Anal. Chim. Acta* **2014**, *838*, 1−12, DOI: 10.1016/j.aca.2014.04.057.
(42) Aghamiri, Z. S.; Mohsennia, M.; Rafiee-Pour, H.-A. Immobilization of Cytochrome c and Its Application as Electrochemical Biosensors. *Talanta* **2018**, *176*, 195−207.
(43) Bilal, M.; Barceló, D.; Iqbal, H. M. Nanostructured Materials for Harnessing the Power of Horseradish Peroxidase for Tailored Environmental Applications. *Sci. Total Environ.* **2020**, *749*, No. 142360.
(44) Yang, B. Y.; Gray, J. S.; Montgomery, R. The Glycans of Horseradish Peroxidase. *Carbohydr. Res.* **1996**, *287*, 203−212.
(45) Correira, J. M.; Webb, L. J. Formation and Characterization of a Stable Monolayer of Active Acetylcholinesterase on Planar Gold. *Langmuir* **2022**, *38*, 3501−3513.
(46) Berglund, G. I.; Carlsson, G. H.; Smith, A. T.; Szoke, H.; Henriksen, A.; Hajdu, J. The Catalytic Pathway of Horseradish Peroxidase at High Resolution. *Nature* **2002**, *417*, 463−468.
(47) Majorek, K. A.; Porebski, P. J.; Dayal, A.; Zimmerman, M. D.; Jablonska, K.; Stewart, A. J.; Chruszcz, M.; Minor, W. Structural and Immunologic Characterization of Bovine, Horse, and Rabbit Serum Albumins. *Mol. Immunol.* **2012**, *52*, 174−182.
(48) Dobbs, A. J.; Anderson, B. F.; Faber, H. R.; Baker, E. N. Three-Dimensional Structure of Cytochrome c' from Two Alcaligenes Species and the Implications for Four-Helix Bundle Structures. *Acta Crystallogr., Sect. D: Biol. Crystallogr.* **1996**, *D52* (2), 356−368.
(49) Booth, M. A.; Kannappan, K.; Hosseini, A.; Partridge, A. In-Depth Electrochemical Investigation of Surface Attachment Chemistry via Carbodiimide Coupling. *Langmuir* **2015**, *31* (29), 8033−8041.
(50) Bartczak, D.; Kanaras, A. G. Preparation of Peptide-Functionalized Gold Nanoparticles Using One Pot EDC/Sulfo-NHS Coupling. *Langmuir* **2011**, *27*, 10119−10123.
(51) Sam, S.; Touahir, L.; Andresa, J. S.; Allongue, P.; Chazalviel, J.; Gouget-Laemmel, A. C.; de Villeneuve, C. H.; Moraillon, A.; Ozanam, F.; Gabouze, N.; Djebbar, S. Semiquantitative Study of the EDC/NHS Activation of Acid Terminal Groups at Modified Porous Silicon Surfaces. *Langmuir* **2010**, *26* (17), 809−814.

https://doi.org/10.1021/acsabm.4c00012
ACS Appl. Bio Mater. XXXX, XXX, XXX−XXX